ENGINEERING TRANSACTIONS • *Engng. Trans.* • **61**, 4, 265–287, 2013
Polish Academy of Sciences • Institute of Fundamental Technological Research (IPPT PAN)
National Engineering School of Metz (ENIM)

Revisiting the Reflected Caustics Method: the Accurate Shape of the "Initial Curve"

Christos F. MARKIDES, Stavros K. KOURKOULIS

National Technical University of Athens, Department of Mechanics, Laboratory of Testing and Materials
5, Heroes of Polytechnion Avenue, 157 73 Zografou Campus, Athens, Greece
e-mail: stakkour@central.ntua.gr

The shape of the "initial curve", i.e. the locus of material points, which if properly illuminated provide (under specific conditions) the "caustic curve", is explored. Adopting the method of complex potentials improved formulae for the shape of the "initial curve" are obtained. Application of these formulae for two typical problems, i.e. the mode-I crack and the infinite plate with a finite circular hole under uniaxial tension, indicates that the "initial curve" is in fact not a circular locus. It is either an open curve or a closed contour, respectively, the actual shape of which depends also on the in-plane displacement field.

Key words: reflected caustics, "initial curve", complex potentials, mode-I crack, stress intensity factor, plate with a circular hole.

1. Introduction

The experimental method of Caustics was first applied for the solution of Fracture Mechanics problems by Manogg in 1964 for transparent materials in the form of "Transmitted Caustics" [1]. A few years later Theocaris broadened the application field of the method by introducing the theory of "Reflected Caustics" [2]. In this way it became possible to study the stress singularity in an elastic plate, irrespectively of whether the material of the plate is transparent or opaque. Initially the method was applied under the title "Shadow Optical Technique". It was only in 1971 when Theocaris introduced the term "Method of Caustics" (from the ancient Greek word "*καυστική*" originating from the verb "*καίω*" which means "burn") [3].

The underlying principle of the method is that in case a light beam impinges on a specimen at the immediate vicinity of a singularity the transmitted or reflected rays (received on a reference plane parallel to the specimen's plane) will concentrate along a strongly illuminated curve (called "caustic curve") due to

the strong variations of both the thickness and refractive index at the region close to the singularity. It is exactly the shape and dimensions of this illuminated locus that permit quantitative investigation of critical characteristics of the stress field around the singularity, like for example the Stress Intensity Factor (SIF).

Since its introduction, the method of caustics has been used by many researchers, as analytically described by KALTHOFF [4] in his concise review paper. From the very first period of its development the application of the method covered a wide field of static engineering problems ranging from the calculation of SIFs (in either isotropic [5] or anisotropic materials [6]) to the determination of material properties [7, 8] and to the study of contact problems [9] and deformed boundaries [10]. In parallel the method was used to study the behaviour of materials under dynamic loading conditions [11–14]. In the same period ROSAKIS and FREUND [15] applied the method to confront plasticity problems while KIKUCHI and HAMANAKA [16] used caustics for the experimental determination of the J-integral.

Today the method of caustics is still under further development [17, 18] and is widely used to determine the intensity of stress fields around static cracks [17], to study dynamic [18] and impact problems [19], interfacial cracks [20, 21], fatigue [22] and contact problems [23, 24] and recently problems at the nanoscale [25]. Moreover the method is widely applied for the study of anisotropic- [26, 27], transversely isotropic- [28], orthotropic- [29] or even graded- [30] and composite materials [31]. Recently Gdoutos used the method of caustics for quantification of the triaxial effects around crack tips [32]. Finally, it is worth mentioning that Younis introduced applications of the method in engineering education by designing appropriate experiments [33].

Although the method gradually became very popular its application is not yet fully standardized (CARAZO-ALVAREZ and PATTERSON [34] were the first who proposed a standardizing procedure around 1999). Moreover little attention is paid to the quantification of errors and inaccuracies introduced by various factors which can be in general classified into two broad categories related to: (i) the experimental set-up and the specimens and (ii) approximations adopted during the development of the theory and the derivation of the respective formulae.

For the first category THEOCARIS and RAZEM [35], already from 1981, attempted a quantification of the errors due to the screen position and the specimen's thickness. Later ROSSMANITH [36] studied the errors due to irregular specimen thickness. A more systematic approach to the problem was presented by WALLHEAD *et al.* [37] while KONSTA-GDOUTOS and GDOUTOS [38] introduced useful guidelines for the correct application of the method setting also the respective applicability limits.

In the second category the most systematic study was that by ROSAKIS and ZEHNDER [39] who developed the exact mapping equations describing reflected

caustics. They pointed out that if the SIFs are evaluated by caustics according to the approximate analysis the errors could be as large as 15%. The accuracy of the method was also assessed by SPYROPOULOS [40] who pointed out that only the exact expressions of the complex potentials should be employed since in case approximate formulae are used errors slip into the results shadowing the actual phenomena.

In the direction of further improving the accuracy of the method an attempt is here presented to eliminate an additional source of errors related to the "initial curve". This term designates the geometric locus of the plate's points which under specific conditions [2, 4] provide the set of reflected rays forming the caustic curve on the screen. The "initial curve" depends on the optical constants of the material and it is not the same for reflections from the rear and the front face of the plate. Moreover it depends on the type of light bundle impinging on the plate (parallel, converging or diverging light rays) as well as on the optical arrangement.

The study is focused to the Reflected Caustics method. Disregarding the discussion about the conditions that must be fulfilled in order for the points of the "initial curve" to provide a caustic curve, attention is paid to the fact that light rays impinge on an already deformed plate. Therefore it appears reasonable to derive the equations of the "initial curve" by considering the deformed state contrary to what is commonly adopted in the classic literature about caustics where the "initial curve" is described ignoring the in-plane deformation (assuming in fact that the magnitude of displacements is negligible with respect to the size of the "initial curve" itself). The approach here described is relieved from this restriction and improved formulae are obtained for the "initial curve". These formulae are then applied in two configurations widely studied by employing the method of caustics, i.e. (i) the mode-I crack and (ii) the infinite plate with a finite circular hole under uniaxial tension at infinity. The results of the analysis indicate that for stiff materials the classic approach (i.e. considering the "initial curve" a circular locus of points on the undeformed specimen) is quite satisfactory even in the presence of strong singularities like crack tips. On the contrary, in case of materials with increased compliance the discrepancy between the two approaches becomes non-negligible, exceeding even 12%.

2. The "initial curve" according to the classic approach [2]

A parallel light beam (planar wave-fronts) impinges normally on a thin plate of thickness t, which is in equilibrium under a system of external in-plane loads F (Fig. 1). Due to lateral deformation of the plate's initially plane surface the light rays reflected form spherical wave-fronts $S(x, y, z)$ the gradient $\boldsymbol{\nabla} S$ of which

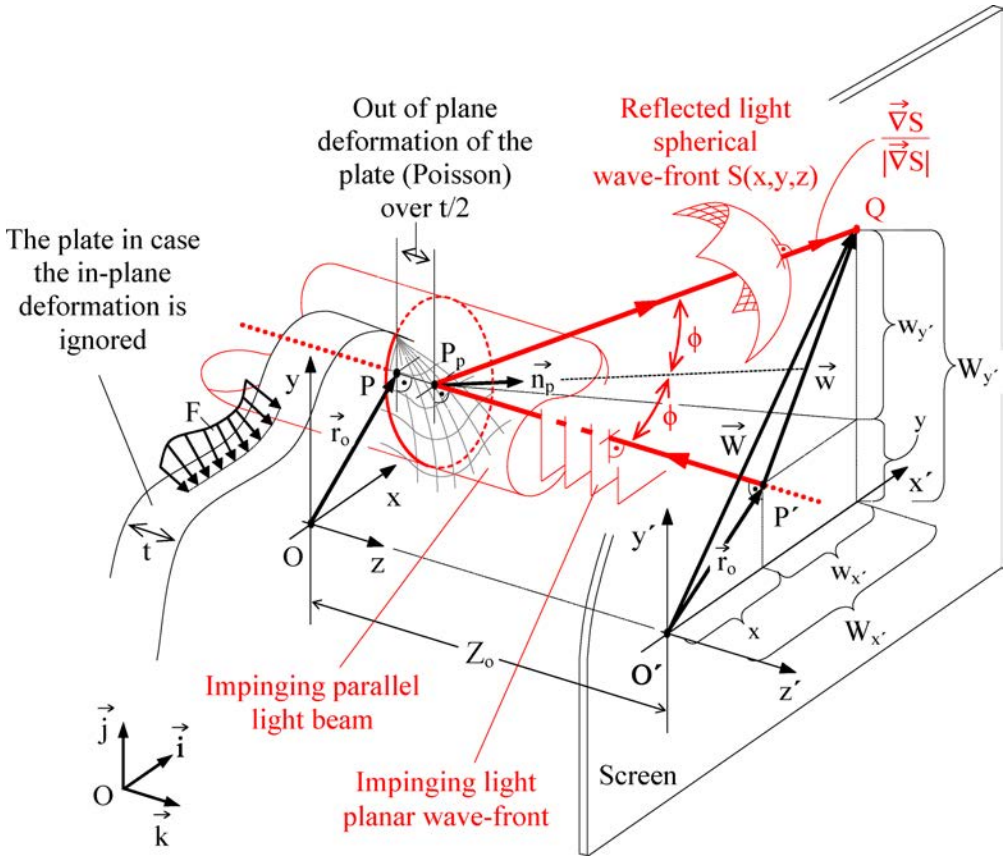

FIG. 1. The classic approach to the formation of the caustic curve from reflected light rays.

at any point is parallel to the respective reflected light ray. The reflected rays impinge on a screen parallel to the plate at a distance Z_o. In case light is reflected from points P (actually from P_p, which is P after the out of plane deformation) with severe lateral deformation a strongly illuminated locus of points Q is formed on the screen (the intersection of the three dimensional surface $S(x, y, z)$ with the screen), called the caustic curve.

According to the classic approach to the Reflected Caustics method [2, 4] two Cartesian reference systems $\{O; x, y, z\}$ and $\{O'; x', y', z'\}$ are considered: One on the front face of the undeformed plate and one on the screen, respectively. The xy- and $x'y'$-planes coincide with the faces of the plate and the screen as it is shown in Fig. 1. Assume now that $P(x, y)$ is a point on the undeformed plate's front face corresponding to a point of deflection (i.e. the normal $\mathbf{n}_p$ to the out of plane-deformed face at P – or strictly speaking at P_p – subtends an angle $\phi \neq 0°$ with the vector normal to the initially planar plate). Assume also

that P' is the normal projection of P on the screen. Then according to Snell's law rays impinging on P_p (or on P considering the negligible magnitude of the out of plane deformation at P with respect to the distance Z_o) are reflected at an angle 2ϕ and the vector $\mathbf{W}$ defines the image Q of P on the caustic curve (Fig. 1). It holds that:

$$\mathbf{W} = \mathbf{r}_o + \mathbf{w} = \mathbf{r}_o + Z_o \boldsymbol{\nabla} s(x, y). \tag{2.1}$$

Vector $\mathbf{r}_o$ corresponds to point P while vector $\mathbf{w} = Z_o \boldsymbol{\nabla} s(x, y)$ describes the deviation of light rays on the screen due to the distortion of the plate at point P. Moreover $s(x, y)$ is the path change of the light rays. Furthermore for Eq. (2.1) to be valid self-similarity for the reflected wave-fronts has been assumed (parallel bent fronts rather than the exact spherical ones [39]):

$$S(x, y, z) = z + s(x, y) = \mathcal{C}_1, \tag{2.2}$$

where $\mathcal{C}_1$ is a constant. Equation (2.2) is valid for small deflection angles ϕ, an assumption well acceptable within the frame of Linear Elasticity. Along the same line of thought it is assumed that:

$$s(x, y) \approx \Delta t(x, y) = \frac{\nu t}{E}(\sigma_1 + \sigma_2). \tag{2.3}$$

In Eq. (2.3) $\Delta t(x, y)$ is the thickness change of the plate (due to the out of plane deformation of the plate) at point P expressed (through Hooke's generalized law) in terms of the principal stresses, σ_1 and σ_2, Poisson's ratio ν, and Young's modulus E. The sum of the two principal stresses is expressed with the aid of the complex potential $\Phi(z)$ [41] as:

$$\sigma_1 + \sigma_2 = 4\Re\Phi(z), \tag{2.4}$$

$\Re$ denotes the real part and $z = x + iy = re^{i\vartheta}$ is the complex variable (not to be confused with the z coordinate axis). Then it is readily seen that Eq. (2.1) for the caustic curve can be written in the quite convenient complex from:

$$W = z + \underbrace{4Z_o t \overbrace{\frac{\nu}{E}}^{c_f}}_{C} \overline{\Phi'(z)} = z + C\overline{\Phi'(z)}, \tag{2.5}$$

where $z = r_o e^{i\vartheta}$ is to be understood as the point P on the "initial curve", prime denotes first order derivative and over-bar the conjugate complex value. Separating real, $\Re$, from imaginary, $\Im$, parts, in Eq. (2.5), the parametric equations of the caustic curve are written as:

$$W_{x'} = x + C\Re\left\{\overline{\Phi'(z)}\right\}, \qquad W_{y'} = y + C\Im\left\{\overline{\Phi'(z)}\right\}. \tag{2.6}$$

In Eq. (2.6) $W_{x'}$, $W_{y'}$ are the horizontal and vertical components of $\mathbf{W}$ on the screen reference (Fig. 1).

The formation of a caustic curve on the screen is the result of a light singularity. Therefore the Jacobian determinant of the transformation of Eqs. (2.6) must be zeroed leading to:

$$C\left|\Phi''(z)\right| = 1. \tag{2.7}$$

Double prime denotes second order derivative. According to the classical approach and terminology Eq. (2.7) provides the so-called "initial curve" [2, 4], i.e. the locus of points of the front face of the plate, (ignoring the in-plane deformation of the plate), on which the impinging light rays are reflected forming the caustic curve on the screen.

In case of a non-parallel impinging light beam Eqs. (2.6), (2.7) become:

$$W_{x'} = \lambda_m x + C\Re\left\{\overline{\Phi'(z)}\right\}, \qquad W_{y'} = \lambda_m y + C\Im\left\{\overline{\Phi'(z)}\right\}, \tag{2.8}$$

$$C\left|\frac{\Phi''(z)}{\lambda_m}\right| = 1, \tag{2.9}$$

where λ_m is the magnification ratio of the optical setup equal to $(Z_o \pm Z_i)/Z_i$ for a divergent or convergent impinging light beam, respectively; Z_i is the distance of the focus of the divergent or convergent light beam from the loaded plate [4].

3. The accurate shape of the "initial-" and caustic-curves

It is seen that according to the above line of thought the "initial curve" is considered as a locus of points P on the in-plane undeformed face of the plate. In fact only the out of plane deformation has been taken into account while the in-plane displacements field induced by the external loading system is assumed negligibly small compared to the size of the "initial curve" itself. Such an assumption is quite acceptable for stiff materials, however it could lead to erroneous results in the case of increased compliance materials for which the magnitude of the displacement components is not ignorable. Thus it appears necessary to discriminate between the deformed and the undeformed state of the plate since the external load causes (in case of plane stress) both out-of-plane as well as in-plane deformations translating any point P of the face of the undeformed plate to a new position P_d and then to P_p. Indeed as it is shown in Fig. 2, neglecting rigid body displacements, point $P(x, y)$ of the undeformed plate, corresponding to vector $\mathbf{r}_o$, shifts to $P_d(x_d, y_d)$ due to the in-plane deformation of the plate through the $\{u, v\}$ displacements (green line in Fig. 2).

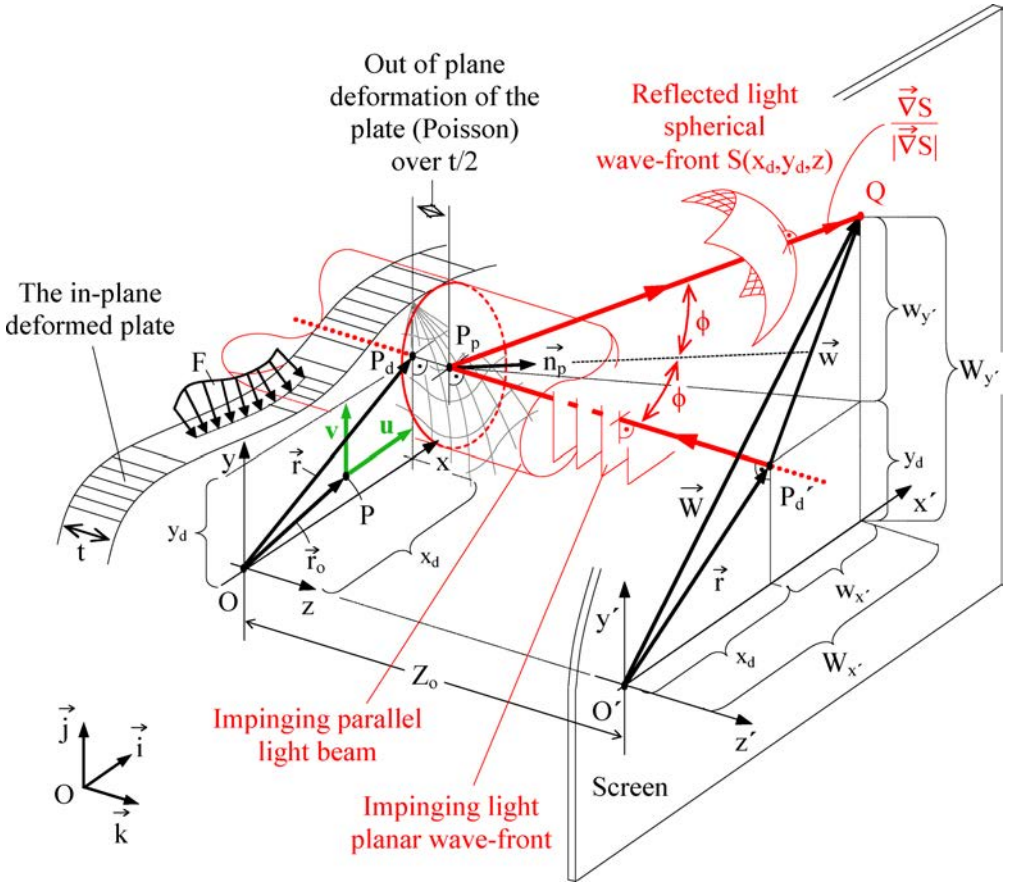

FIG. 2. The improved approach to the formation of the caustic curve from reflected light rays.

Moreover the out of plane deformation $\Delta t(x, y)/2$ of the front face of the plate (due to Poisson's effect) binds P_d to shift to P_p on the deformed surface of the front face. P_d' is the normal projection of P_d as well as P_p on the screen. Then light impinges on P_p and as long as this is a point of deflection its image Q on the screen belongs to the caustic curve. Obviously, as it is mentioned also in the previous paragraph, for an in-plane investigation (and assuming Δt negligible compared with Z_o) points P_d can sufficiently stand instead of points P_p. It is clear that the only difference between the classic approach (described in Fig. 1) and the improved one here introduced (described in Fig. 2) lies only in the fact that in the later the in-plane deformation of the plate through the $\{u, v\}$ displacements is taken also under consideration. Obviously it holds that (Fig. 2):

$$x_d = x + u = x', \qquad y_d = y + v = y'. \tag{3.1}$$

Therefore Eq. (2.1) of the classic approach is modified to:

$$\mathbf{W} = \mathbf{r} + \mathbf{w} = (\mathbf{r}_o + \mathbf{u}) + Z_o \boldsymbol{\nabla} s(x_d, y_d), \qquad \mathbf{u} = u(x,y)\mathbf{i} + v(x,y)\mathbf{j}, \tag{3.2}$$

where u and v are the horizontal and vertical components of the displacement at $P(x,y)$ (Fig. 2), vector $\mathbf{r}$ corresponds to point $P_d(x_d, y_d)$ and $\mathbf{w} = Z_o \boldsymbol{\nabla} s(x_d, x_d)$, $\boldsymbol{\nabla} = \dfrac{\partial}{\partial x_d}\mathbf{i} + \dfrac{\partial}{\partial y_d}\mathbf{j}$. In addition $s(x_d, y_d)$ is the change of the path of light rays in the space between points P_d of the in-plane deformed face of the plate and the reference screen. Assuming again self-similar reflected wave-fronts instead of Eq. (2.2) one should now write:

$$S(x_d, y_d, z) = z + s(x_d, y_d) = \mathcal{C}_2, \tag{3.3}$$

where $\mathcal{C}_2$ is again a constant. Accordingly Eq. (2.3) is rewritten as:

$$s(x_d, y_d) \approx \Delta t(x,y) = \frac{\nu t}{E}(\sigma_1 + \sigma_2). \tag{3.4}$$

Eq. (3.4) differs from Eq. (2.3) in that $s(x,y)$ was substituted by $s(x_d, y_d)$. This substitution is always feasible assuming that s depends only on the out-of-plane deformation Δt. Therefore Δt may equally well be superimposed either to P (undeformed state – classic approach) or to P_d (deformed state – present approach), according to any succession, as long as the principle of superposition is valid. Introducing Eq. (3.4) in $\mathbf{w} = Z_o \boldsymbol{\nabla} s(x_d, x_d)$, leads to:

$$\begin{aligned} \mathbf{w} &= Z_o \left[\frac{\partial \Delta t(x,y)}{\partial x_d}\mathbf{i} + \frac{\partial \Delta t(x,y)}{\partial y_d}\mathbf{j} \right] \\ &= Z_o \left[\frac{\partial \Delta t(x,y)}{\partial x}\frac{\partial x}{\partial x_d}\mathbf{i} + \frac{\partial \Delta t(x,y)}{\partial y}\frac{\partial y}{\partial y_d}\mathbf{j} \right]. \end{aligned} \tag{3.5}$$

For relatively small deformations and taking into consideration Eqs. (3.1) it follows that:

$$\begin{aligned} \frac{\partial x_d}{\partial x} &= \frac{\partial \left[x + u(x,y)\right]}{\partial x} = 1 + \frac{\partial u(x,y)}{\partial x} \approx 1, \\ \frac{\partial y_d}{\partial y} &= \frac{\partial \left[y + v(x,y)\right]}{\partial y} = 1 + \frac{\partial v(x,y)}{\partial y} \approx 1. \end{aligned} \tag{3.6}$$

Therefore Eq. (3.5) is reduced to:

$$\mathbf{w} = Z_o \left[\frac{\partial \Delta t\,(x,y)}{\partial x}\mathbf{i} + \frac{\partial \Delta t\,(x,y)}{\partial y}\mathbf{j} \right] \tag{3.7}$$

which is found to be identical to the respective formula obtained for **w** according to the classic approach. In turn Eq. (2.5) is now written as:

$$W = z + u + iv + C\overline{\Phi'(z)} \tag{3.8}$$

while the parametric equations of the caustic curve (Eqs. (2.6) of Sec. 2) become:

$$\begin{aligned} W_{x'} &= x_d + C\Re\left\{\overline{\Phi'(z)}\right\} = x + u + C\Re\left\{\overline{\Phi'(z)}\right\}, \\ W_{y'} &= y_d + C\Im\left\{\overline{\Phi'(z)}\right\} = y + v + C\Im\left\{\overline{\Phi'(z)}\right\}. \end{aligned} \tag{3.9}$$

Again, as in Sec. 2 the Jacobian of the transformation between the plate (considered now under in-plane deformation also) and the screen must be zeroed. In other words:

$$J = \begin{vmatrix} \dfrac{\partial W_{x'}}{\partial x_d} & \dfrac{\partial W_{x'}}{\partial y_d} \\ \dfrac{\partial W_{y'}}{\partial x_d} & \dfrac{\partial W_{y'}}{\partial y_d} \end{vmatrix} = 0. \tag{3.10}$$

Due to the Cauchy-Riemann conditions, it holds that:

$$\Re\left\{\overline{\Phi'(z)}\right\} = \frac{\partial\Re\{\Phi(z)\}}{\partial x}, \qquad \Im\left\{\overline{\Phi'(z)}\right\} = \frac{\partial\Re\{\Phi(z)\}}{\partial y} \tag{3.11}$$

and taking into account Eqs. (3.6), the Jacobian's elements become:

$$\begin{aligned} \frac{\partial W_{x'}}{\partial x_d} &= 1 + C\frac{\partial\Re\left\{\overline{\Phi'(z)}\right\}}{\partial x_d} = 1 + C\frac{\partial^2\Re\{\Phi(z)\}}{\partial x^2}\frac{\partial x}{\partial x_d} = 1 + C\frac{\partial^2\Re\{\Phi(z)\}}{\partial x^2}, \\ \frac{\partial W_{x'}}{\partial y_d} &= C\frac{\partial\Re\left\{\overline{\Phi'(z)}\right\}}{\partial y_d} = C\frac{\partial^2\Re\{\Phi(z)\}}{\partial x\partial y}\frac{\partial y}{\partial y_d} = C\frac{\partial^2\Re\{\Phi(z)\}}{\partial x\partial y}, \\ \frac{\partial W_{y'}}{\partial x_d} &= C\frac{\partial\Im\left\{\overline{\Phi'(z)}\right\}}{\partial x_d} = C\frac{\partial^2\Re\{\Phi(z)\}}{\partial y\partial x}\frac{\partial x}{\partial x_d} = C\frac{\partial^2\Re\{\Phi(z)\}}{\partial x\partial y}, \\ \frac{\partial W_{y'}}{\partial y_d} &= 1 + C\frac{\partial\Im\left\{\overline{\Phi'(z)}\right\}}{\partial y_d} = 1 + C\frac{\partial^2\Re\{\Phi(z)\}}{\partial y^2}\frac{\partial y}{\partial y_d} = 1 + C\frac{\partial^2\Re\{\Phi(z)\}}{\partial y^2}, \end{aligned} \tag{3.12}$$

whence

$$C\left|\Phi''(z)\right| = 1. \tag{3.13}$$

At this point it is worth mentioning that Eq. (3.13) is identical to Eq. (2.7), as a direct consequence of Eqs. (3.6) holding for the relatively small deformations considered here. However there is a critical difference between the two approaches lying in the fact that according to the classic one Eq. (2.7) is the "initial curve" itself while according to the present one Eq. (2.7) or Eq. (3.13) describes the locus of points z (or P) on the undeformed plate to which one should add the respective displacements $\{u, v\}$ in order to obtain the actual "initial curve" (in the sense that the later lies on the deformed face of the plate rather than on the undeformed one).

In case of a divergent or convergent light beam, i.e. for $\lambda_m \neq 1$, Eqs. (3.9), (3.13) become:

$$\begin{aligned} W_{x'} &= \lambda_m x_d + C\Re\left\{\overline{\Phi'(z)}\right\} = \lambda_m(x+u) + C\Re\left\{\overline{\Phi'(z)}\right\}, \\ W_{y'} &= \lambda_m y_d + C\Im\left\{\overline{\Phi'(z)}\right\} = \lambda_m(y+v) + C\Im\left\{\overline{\Phi'(z)}\right\}, \end{aligned} \tag{3.14}$$

$$C\left|\frac{\Phi''(z)}{\lambda_m}\right| = 1. \tag{3.15}$$

Again Eq. (3.15) is identical to Eq. (2.9) while Eqs. (3.14) represent the improved version of Eqs. (2.8) of the classic approach.

4. Applications

Two typical problems, widely studied by employing the method of Reflected Caustics, are here revisited in order to reveal the main features of the present approach and also to quantify the difference from the classic approach:

(i) The mode-I crack.

(ii) The infinite plate with a circular hole under tension.

4.1. The mode-I crack

The configuration of the problem and the optical setup in case of parallel light impinging normally to the plate ($\lambda_m = 1$) are shown in Fig. 3. The initial (undeformed) crack (thin lines) of length 2α opens symmetrically with respect to its axis due to the uniaxial tension σ_o at infinity. The origin of the coordinate axes is the crack tip. The complex potentials for the singular solution are [41]:

$$\left.\begin{matrix}\Phi(z)\\ \Omega(z)\end{matrix}\right\} = \frac{\sigma_o}{2}\left(\sqrt{\frac{\alpha}{2z}} \mp \frac{1}{2}\right), \qquad \left.\begin{matrix}\varphi(z)\\ \omega(z)\end{matrix}\right\} = \frac{\sigma_o}{2}\left(\sqrt{2\alpha z} \mp \frac{\alpha+z}{2}\right), \tag{4.1}$$

whence

$$\left|\Phi''(z)\right| = \frac{3\sigma_o}{8}\sqrt{\frac{\alpha}{2}}\frac{1}{r^{5/2}}. \tag{4.2}$$

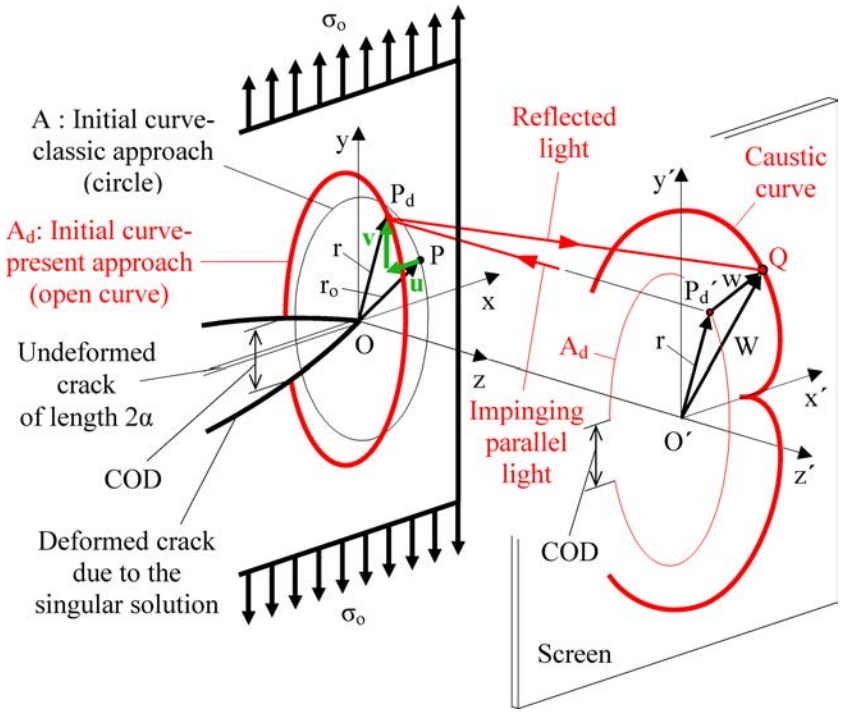

FIG. 3. Reflected caustic curve due to a crack tip according to the present approach.

The deformed (opened) lips of the crack, due to the singular solution, are shown with a bold line in Fig. 3. According to the classic approach points $P(x, y)$ (or in complex form $z = r_o e^{i\vartheta}$) of the undeformed plate forming the "initial curve" are obtained through Eq. (2.9) as:

$$r_o = \left(\frac{3C\sigma_o}{8\,|\lambda_m|} \sqrt{\frac{\alpha}{2}} \right)^{2/5}. \tag{4.3}$$

Clearly due to Eq. (4.3) the "initial curve" is a (closed) circle denoted by A (thin line) in Fig. 3 (Fig. 3 refers to the case with $\lambda_m = 1$). According to the present approach in order to obtain the actual "initial curve" the displacement field of points P (on A) have to be added to the circle A. Taking advantage of the well-known formula [41]:

$$2\mu(u + iv) = \kappa\phi(z) - \omega\,(\overline{z}) - (z - \overline{z})\,\overline{\Phi(z)}, \tag{4.4}$$

(κ is Muskhelishvili's constant and μ the shear modulus of the plate's material) one obtains with the aid of Eqs. (4.1) the components of the displacement of points P (or $z = r_o e^{i\vartheta}$) on A as:

$$u = \frac{\sigma_o}{2\mu}\left[(\kappa-1)\sqrt{\frac{\alpha r_o}{2}}\cos\frac{\vartheta}{2} - \frac{\kappa+1}{4}(\alpha + r\cos\vartheta) - \frac{1}{2}\sqrt{\frac{\alpha r_o}{2}}\left(\cos\frac{3\vartheta}{2} - \cos\frac{\vartheta}{2}\right)\right],$$

$$v = \frac{\sigma_o}{2\mu}\left[(\kappa+1)\sqrt{\frac{\alpha r_o}{2}}\sin\frac{\vartheta}{2} - \frac{\kappa-1}{4}r\sin\vartheta - \frac{1}{2}\sqrt{\frac{\alpha r_o}{2}}\left(\sin\frac{3\vartheta}{2} + \sin\frac{\vartheta}{2}\right)\right]. \tag{4.5}$$

Then by adding the above u and v (green line in Fig. 3) to points P of Eq. (4.3) on A one obtains points P_d on the actual, according to the present approach, "initial curve" A_d of varying radius r. As it is shown in Fig. 3, the "initial curve" A_d (red bold line), referred to the deformed plate, is not a closed circle but an elliptic not closed curve due to the crack opening displacement. In Fig. 3 also the projection of A_d on the screen has been drawn (red thin line). Moreover according to the classic approach the parametric equations of the caustic curve are obtained through Eqs. (2.8) (for $\lambda_m \neq 1$) as follows:

$$W_{x'} = \lambda_m r_o\left(\cos\vartheta - \frac{2}{3}\cos\frac{3\vartheta}{2}\right), \qquad W_{y'} = \lambda_m r_o\left(\sin\vartheta - \frac{2}{3}\sin\frac{3\vartheta}{2}\right), \tag{4.6}$$

while according to the present approach Eqs. (3.14) in combination with Eqs. (4.5) yield the parametric equations for point Q on the caustic curve (red bold line on the screen Fig. 3) as:

$$W_{x'} = \lambda_m r_o\left\{\left(\cos\vartheta - \frac{2}{3}\cos\frac{3\vartheta}{2}\right) + \frac{\sigma_o}{2\mu}\left[(\kappa-1)\sqrt{\frac{\alpha}{2r_o}}\cos\frac{\vartheta}{2} - \frac{\kappa+1}{4}\left(\frac{\alpha}{r_o} + \cos\vartheta\right) - \frac{1}{2}\sqrt{\frac{\alpha}{2r_o}}\left(\cos\frac{3\vartheta}{2} - \cos\frac{\vartheta}{2}\right)\right]\right\},$$

$$W_{y'} = \lambda_m r_o\left\{\left(\sin\vartheta - \frac{2}{3}\sin\frac{3\vartheta}{2}\right) + \frac{\sigma_o}{2\mu}\left[(\kappa+1)\sqrt{\frac{\alpha}{2r_o}}\sin\frac{\vartheta}{2} - \frac{\kappa-1}{4}\sin\vartheta - \frac{1}{2}\sqrt{\frac{\alpha}{2r_o}}\left(\sin\frac{3\vartheta}{2} + \sin\frac{\vartheta}{2}\right)\right]\right\}. \tag{4.7}$$

The "initial curves" obtained according to the two approaches considered (the classic and the present one) are plotted in juxtaposition in Fig. 4. Dotted line corresponds to the circular "initial curve" of the classic approach while the continuous one to the improved version. For plotting Fig. 4 plane stress conditions were assumed for a rectangular centrally cracked plate (made from PCBA with Young's modulus $E = 2.5$ GPa and Poisson's ratio $\nu = 0.38$) of

length $\ell = 0.10$ m, thickness $t = 2$ mm, and half crack length $\alpha = 0.01$ m. The plate is subjected to a tensile stress at infinity equal to one fifth of the yield stress acting normally to the crack axis. The magnification factor λ_m was set equal to 4. As it is seen from Fig. 4 the improved version of the "initial curve" is slightly displaced inwards, with respect to the crack tip, without being self-similar with the approximate one. Moreover it is discontinuous since the initial crack is no longer a mathematic line, but rather it's two lips are at a finite distance from each other and equal to the crack opening displacement at the point where the "initial curve" intersects the crack boundaries. Although the differences are rather small from a quantitative point of view they significantly change the data obtained from the respective caustic curves.

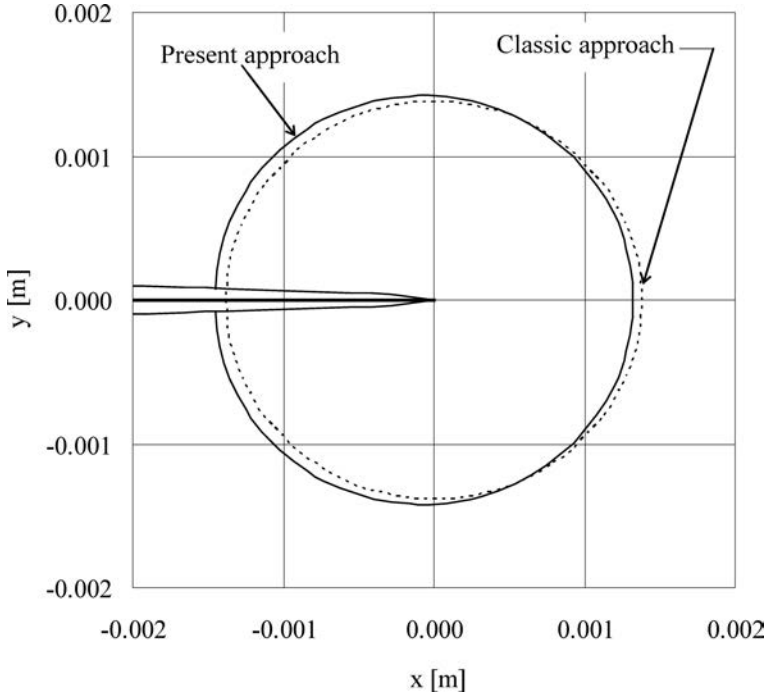

FIG. 4. The "initial curve" in case of the two approaches considered. Dotted line represents the approximate circular "initial curve" (classic approach) while the continuous line corresponds to the exact shape according to the present approach.

For the above statement to be verified, the two caustic curves obtained from Eqs. (4.6) and (4.7) (for the same numerical data as previously), are plotted in Fig. 5. It is seen that the caustic curve obtained from the accurate "initial curve" encompasses that obtained from the classic circular "initial curve" for the major $[-\pi, \pi]$ region. For the differences to be quantified the distance between the two tangents to the caustic curve parallel to the crack axis are compared in

Fig. 5. This distance is usually denoted as $D_1^{\min}$. As it can be seen from Fig. 5 the distance $D_1^{\min}{}_{,P}$ obtained from the present approach exceeds $D_1^{\min}{}_{,C}$ of the classic approach, by about 5.5%. Taking into account the proof by Theocaris and Pazis [42] (based on the general theory of epicycloid curves), that $D_1^{\min}$ is directly related to the stress intensity factor through the formulae [42]:

$$K_I \sim \sqrt[2]{\left(D_1^{\min}\right)^5} \tag{4.8}$$

it is easily concluded that the mode-I stress intensity factors K_I calculated according to the two approaches differ by more than 12%.

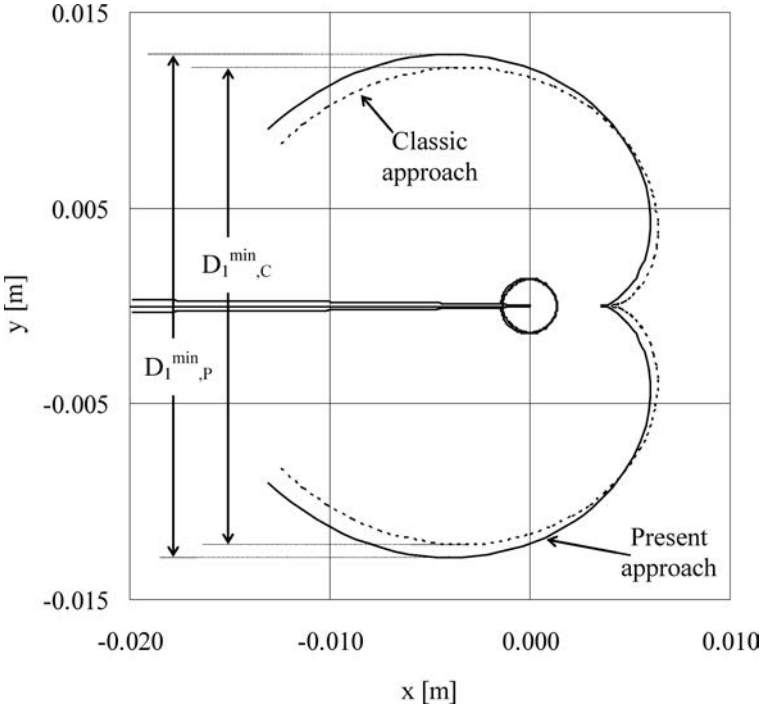

FIG. 5. The caustic curves, dotted and continuous lines, in case of a strong singularity (crack tip) as obtained from light rays reflected on the approximate and on the exact) "initial curves", respectively.

4.2. The infinite plate with a finite circular hole under uniaxial tension at infinity

The configuration of the problem and the optical setup in case of parallel light impinging normally to the plate ($\lambda_m = 1$) are shown in Fig. 6. The initial (undeformed) hole (thin line) of radius R deforms to an ellipse (bold line) due to the uniaxial tension σ_o at infinity. The origin of the coordinate system is

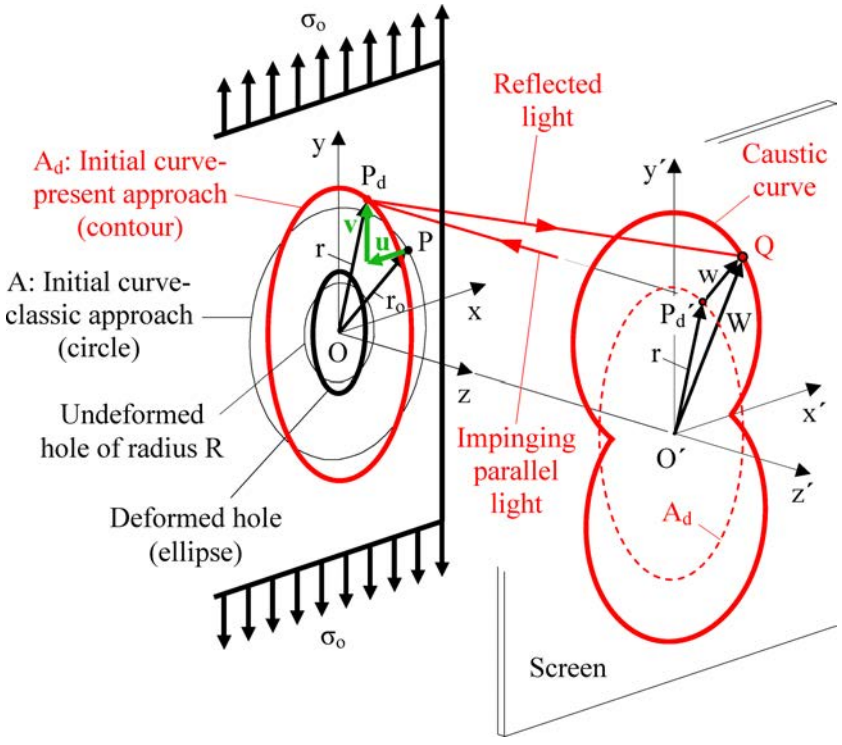

FIG. 6. Reflected caustic curve due to a circular hole according to the present approach.

the centre of the hole. The complex potentials required for the solution of the problem are [41]:

$$\Phi(z) = \frac{\sigma_o}{4}\left(1 + \frac{2R^2}{z^2}\right), \qquad \varphi(z) = \frac{\sigma_o}{4}\left(z - \frac{2R^2}{z}\right),$$
$$\psi(z) = \frac{\sigma_o}{2}\left(z - \frac{R^2}{z} - \frac{R^4}{z^3}\right), \tag{4.9}$$

whence

$$\left|\Phi''(z)\right| = \frac{3\sigma_o R^2}{r^4}. \tag{4.10}$$

Again according to the classic approach points $P(x, y)$ (or $z = r_o e^{i\vartheta}$) of the undeformed plate forming the "initial curve" are obtained through Eq. (2.9) as:

$$r_o = \left(\frac{3C\sigma_o R^2}{|\lambda_m|}\right)^{1/4} \tag{4.11}$$

Eq. (4.11) is in fact the equation of a circle, denoted by A (thin line) in Fig. 6 (Fig. 6 refers to the case $\lambda_m = 1$). On the contrary according to the present approach the actual "initial curve" follows from A by adding the displacement field of points P (on A).

In this direction, employing Muskhelishvili's formula [41]:

$$2\mu\,(u+iv) = \kappa\varphi(z) - z\overline{\varphi'(z)} - \overline{\psi(z)} \tag{4.12}$$

in combination with Eqs. (4.9) one obtains the components of displacement of points P (or $z = r_o e^{i\vartheta}$) on A as:

$$\begin{aligned} u &= \frac{\sigma_o}{8\mu r_o}\left\{\left[\kappa\left(r_o^2 - 2R^2\right) + 2R^2 - 3r_o^2\right]\cos\vartheta - \frac{2R^2\left(r_o^2 - R^2\right)}{r_o^2}\cos 3\vartheta\right\}, \\ v &= \frac{\sigma_o}{8\mu r_o}\left\{\left[\kappa\left(r_o^2 + 2R^2\right) + 2R^2 + r_o^2\right]\sin\vartheta - \frac{2R^2\left(r_o^2 - R^2\right)}{r_o^2}\sin 3\vartheta\right\}. \end{aligned} \tag{4.13}$$

Adding u and v (green line in Fig. 6) from Eqs. (4.13) to points P of Eq. (4.11) one obtains points P_d on the actual, according to the present approach, "initial curve" A_d (red bold line in Fig. 6) of varying radius r. In Fig. 6 also the projection of A_d on the screen has been drawn (red dotted line).

Moreover according to the classic approach the parametric equations of the caustic curve are obtained through Eqs. (2.8) as:

$$W_{x'} = \lambda_m r_o\left(\cos\vartheta - \frac{1}{3}\cos 3\vartheta\right), \qquad W_{y'} = \lambda_m r_o\left(\sin\vartheta - \frac{1}{3}\sin 3\vartheta\right). \tag{4.14}$$

On the contrary according to the present approach Eqs. (3.14) in combination with Eqs. (4.13) yield the parametric equations for point Q on the caustic curve (red bold line on the screen Fig. 6) as:

$$\begin{aligned} W_{x'} &= \lambda_m r_o\left\{\left(\cos\vartheta - \frac{1}{3}\cos 3\vartheta\right)\right. \\ &\quad \left. + \frac{\sigma_o}{8\mu}\left\{\left[\kappa\left(1 - \frac{2R^2}{r_o^2}\right) + \frac{2R^2}{r_o^2} - 3\right]\cos\vartheta - \frac{2R^2\left(r_o^2 - R^2\right)}{r_o^4}\cos 3\vartheta\right\}\right\}, \\ W_{y'} &= \lambda_m r_o\left\{\left(\sin\vartheta - \frac{1}{3}\sin 3\vartheta\right)\right. \\ &\quad \left. + \frac{\sigma_o}{8\mu}\left\{\left[\kappa\left(1 + \frac{2R^2}{r_o^2}\right) + \frac{2R^2}{r_o^2} + 1\right]\sin\vartheta - \frac{2R^2\left(r_o^2 - R^2\right)}{r_o^4}\sin 3\vartheta\right\}\right\}. \end{aligned} \tag{4.15}$$

Considering again a PCBA plate of the same as previously dimensions and mechanical properties with a central circular hole of radius $R = 0.01$ m one

can plot the caustic curves due to the classic (Eqs. (4.14)) and the present (Eqs. (4.15)) approaches as it is seen in Fig. 7 (only one quarter of the plate is plotted for double symmetry reasons). Obviously the differences are less striking given that the singularity is now weaker (compared to the crack tip). However even in this case there is an increase of the maximum transverse dimension of the caustic (denote as D_m in Fig. 7) equal to about 2.5%.

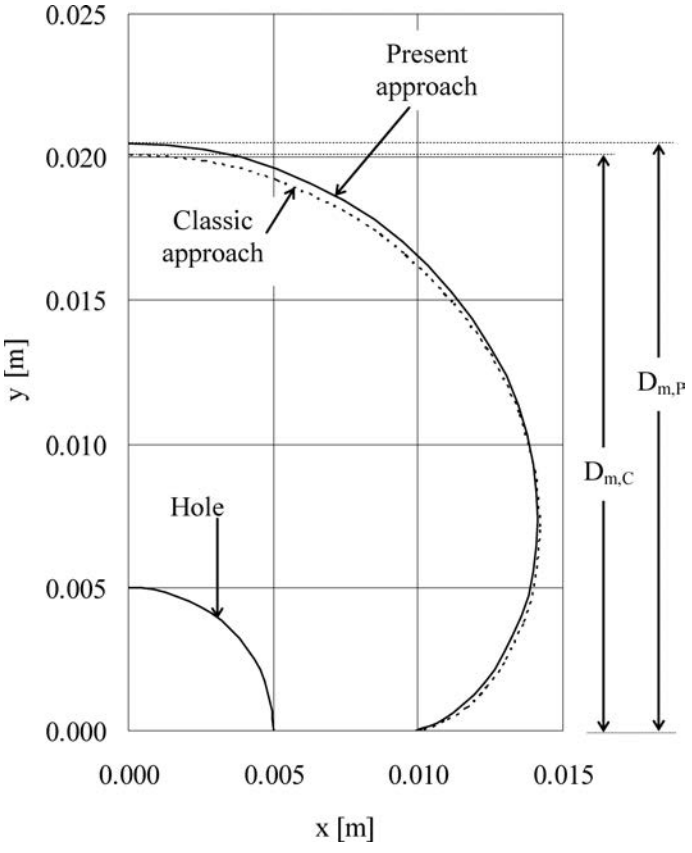

FIG. 7. The caustic curves, dotted and continuous lines, in case of a weak singularity (circular hole) as obtained from light rays reflected on the approximate and the exact "initial curves", respectively.

Recalling the familiar formula [43]:

$$\sigma_o \sim D_m^4 \tag{4.16}$$

which relates the stress induced at infinity σ_o to the characteristic dimension of the caustic, differences of the order of 10% are obtained for σ_o if it is calculated according to the two approaches here considered.

5. Discussion and conclusions

The experimental method of caustics, either transmitted or reflected, is considered nowadays a useful and flexible tool for the exploration of specific features of the stress field around singularities due to its sensitivity to deformation gradients. Despite the fact that the method was introduced almost fifty years ago, it is not yet standardized and a few questions are still open concerning its natural foundation, the optimum procedure for its application, as well as the assessment of the experimental results. Despite these open questions the method is nowadays widely used in various modern fields of experimental strength of materials (as it was mentioned in the introductory section) covering both mechanical- (i.e. roller bearing contact [44]) and civil-engineering applications (i.e. behaviour of rocks under impact [45]).

The present study was devoted to the determination of the accurate shape of the "initial curve" without falling back on the assumption that the deformation field is negligible compared to the size of the "initial curve". The importance of the correct determination of the "initial curve" is better understood taking into account that all points of the "initial curve" are mapped onto the caustic curve while all points inside and outside this curve are mapped outside the caustic. Considering that the light rays forming the caustic curve originate exclusively from the "initial curve", it is understood that all information gathered from the caustic curve depends exclusively on the respective "initial curve". The significance of the "initial curve" is further accentuated considering that by varying Z_o (changing for example the focal plane of the recording system), the position of the "initial curve" varies accordingly, permitting a scanning of the near-tip region enlightening critical features of the stress field surrounding the singularity.

In this direction closed-form formulae for the actual shape of the "initial curve" were deduced. Taking advantage of these formulae the caustic curves formed by light rays reflected at the points of the actual "initial curve" were drawn and compared with the respective ones corresponding to a circular "initial curve" on the undeformed plate. Both qualitative and quantitative differences between the two approaches (the approximate classic one and the more accurate one proposed here) were detected which are essentially independent from both the kind of light bundle impinging on the plate (parallel, converging or diverging light rays) and also from the experimental setup. From a quantitative point of view the importance of these differences depends on the nature of the specimen's material. In fact for brittle and relatively stiff materials like PMMA the differences quantified between the two approaches are either negligible (for weak singularities like the circular hole) or they fall well within experimental error (i.e. less than 4%) for strong singularities (like the crack tip). On the contrary for less stiff materials like PCBA the differences are of the order of 10% or even

higher for both weak and strong singularities. Obviously differences of the order here detected should not be ignored for either weak or strong singularities.

A quantitative overview of this point is gained from Fig. 8 where the percentage difference between the classic and the present approaches is plotted versus the elastic modulus of a wide class of real materials ranging from stiff ones (a type of soft rock) to materials with increased compliance (PTFE). Both the cases of weak (hole in an infinite plate) and strong (mode-I crack) singularities are described. For comparison reasons in the case of a weak singularity the load induced was equal to one third of the respective yield stress while for the strong singularity the stress at infinity was one fifth of the respective yield one. Both the raw data (characteristic dimension of the caustic curve) and the quantities obtained from these data (mode-I stress intensity factor K_I and stress at infinity σ_o) are plotted in Fig. 8, clearly supporting the conclusions drawn in the previous paragraphs.

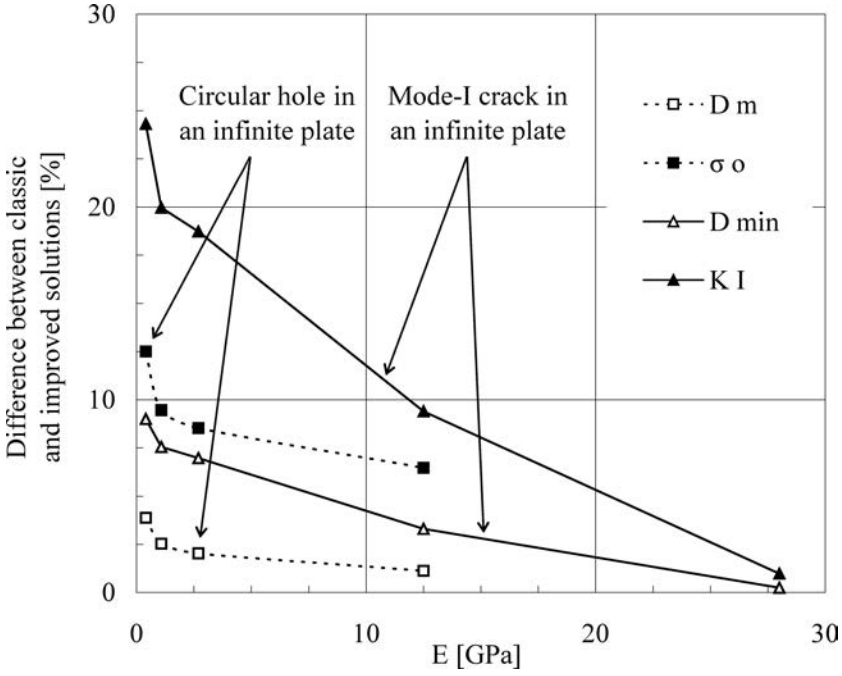

FIG. 8. The difference between the two approaches versus the elastic modulus of the specimens' material. Triangular symbols correspond to the strong singularity while the rectangular ones to the weak singularity. Empty symbols represent the raw data obtained directly from the caustic while the filled ones correspond to the indirectly calculated quantities.

Before concluding it is once again emphasized that the approach introduced here assumes relatively small deformations, as it is in the case of the classic approach. The difference lies in that the classic approach ignores both the gra-

dients of the in-plane displacements and the in-plane displacements themselves. On the contrary, in the present approach only the gradients of the displacement field were ignored while the displacements themselves were taken into account. This could be proved very beneficial in specific applications such as for example, the determination of the contact length in case of two elastic bodies in contact using the method of reflected caustics. In such a case where the quantity to be determined (contact length) is well comparable to the dimensions of the displacement field's components it is obvious that ignoring the displacement components themselves is erroneous. The specific problem for the case of two elastic discs (radius $R = 50$ mm and thickness $t = 10$ mm) made of PMMA and compressed against each other along a common generatrix of their external surfaces was recently solved analytically [46] according to the improved approach introduced in Sec. 4. Characteristic results of this analysis are shown in Fig. 9, where the

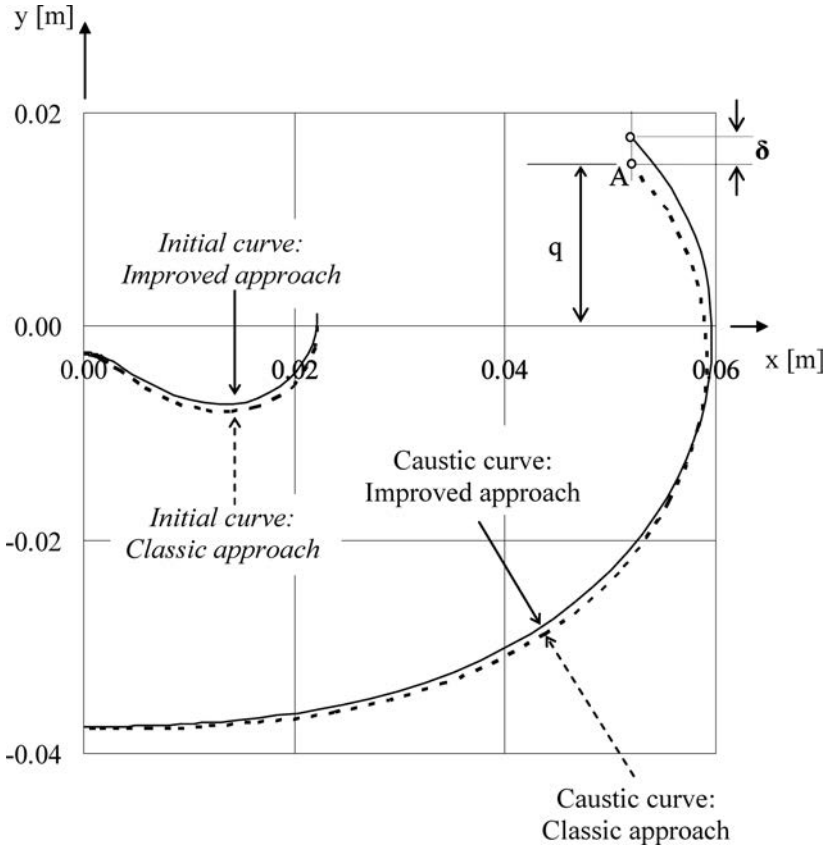

FIG. 9. The "initial curves" and the respective caustics obtained from the contact area of two discs compressed against each other along a common generatrix of their external surface. Dotted lines represent the classic formulation while the continuous ones correspond to the present approach.

"initial curves" and the respective contact caustics are plotted according to both the classic and the improved approaches. According to the theoretical analysis described in detail in ref. [46] the "elevation" q of the end-points A of the caustic curve is directly related to the length of the contact arc developed between the two discs. As it can be seen from Fig. 9, the difference δ of the elevation determined by employing the classic and the improved approaches of the reflected caustics method exceeds 15%. Obviously in case the discs were made from a less stiff material (like for example PTFE or PCBA) the difference would become higher rendering the results of the classic approach unreliable.

Acknowledgment

The authors express their sincere gratitude to Professor D.N. Pazis of the Department of Mechanics of the National Technical University of Athens. His deep knowledge on the founding principles of the method of caustics and his unique experience on its laboratory application were unsparingly offered and greatly contributed to the final outcome of the present research.

References

1. Manogg P., *Schattenoptische Messung der spezifischen Bruchenergie waehrend des Bruchvorgangs bei Plexiglas*, Proceedings of the International Conference on Physics of Noncrystalline Solids, Prins J.A. [Ed.], Delft, The Netherlands, 481–490, 1964.
2. Theocaris P.S., *Local Yielding Around a Crack-Tip in Plexiglas*, Journal of Applied Mechanics, **37**, 409–415, 1970,
3. Theocaris P.S., *The Constrained Zones in Collinear Asymmetric Cracks by the Method of Caustics*, Proceedings of the 7th All Union Conference on Photoelasticity, Tallinn, November 1971, **2**, 221–236, 1971.
4. Kalthoff J.F., *Shadow optical method of caustics*, Handbook of Experimental Mechanics, Kobayashi A.S. [Ed.], Prentice-Hall, New York, pp. 430–498, 1987.
5. Theocaris P.S., Gdoutos E.E., *An optical method for determining opening-mode and edge sliding-mode stress intensity factors*, Journal of Applied Mechanics, **39**, 91–97, 1972.
6. Rossmanith H.P., *General mode-1 caustic evaluation for optically anisotropic materials*, Archive of Applied Mechanics, **50**, 73–83, 1981.
7. Theocaris P.S., Ioakimidis N.I., *Application of the method of caustics to the determination of the ratio of Poisson's ratio to the modulus of elasticity*, Journal of Physics D: Applied Physics, **12**, 1321–1324, 1979.
8. Younis N.T., Zachary L.W., *A new technique for the determination of stress-optical constants using the shadow spot method*, Experimental Mechanics, **29**, 75–79, 1989.
9. Theocaris P.S., *Experimental study of plane elastic contact problems by the pseudocaustics method*, Journal of Mechanics and Physics of Solids, **27**, 15–32, 1979.
10. Theocaris P.S., Razem C., *Deformed boundaries determined by the method of caustics*, The Journal of Strain Analysis for Engineering Design, **12**, 223–232, 1977.

11. Kalthoff J.F., Winkler S., Beinert J., *Dynamic SIFs for arresting cracks in DCB Specimens*, International Journal of Fracture, **12**, 317–319, 1976.

12. Theocaris P.S., Andrianopoulos N.P., *Dynamic three-point bending of short beams studied by caustics*, International Journal of Solids and Structures, **17**, 707–715, 1981.

13. Papadopoulos G.A., *Dynamic Caustics and its Applications*, Optics and Lasers in Engineering, **13**, 211–249, 1990.

14. Georgiadis H.G., Papadopoulos G.A., *On the method of dynamic caustics in crack propagation experiments*, International Journal of Fracture, **54**, R19–R22, 1992.

15. Rosakis A.J., Freund L.B., *Optical measurements of the plastic strain concentration at a tip in a ductile steel plate*, Journal of Engineering Materials and Technology (Transactions of the ASME), **104**, 115–125, 1982.

16. Kikuchi M., Hamanaka S., *Evaluation of the J-Integral by the Caustics Method*, Transactions of the Japan Society of Mechanical Engineers A, **56**(532), 2581–2587, 1990.

17. Papadopoulos G.A., *New formula of experimental stress intensity factor evaluation by caustics*, International Journal of Fracture, **171**, 79–84, 2011.

18. Yao Xuefeng, Xu Wei, *Recent application of caustics on experimental dynamic fracture studies*, Fatigue & Fracture of Engineering Materials & Structures, **34**, 448–459, 2011.

19. Yao Xuefeng, Xu Wei, Jin Guan Chang, Yeh Hsien Yang, *Low velocity impact study of laminate composites with mode I crack using dynamic optical caustics*, Journal of Reinforced Plastics and Composites, **23**, 1833–1844, 2004.

20. Xiong Chunyang, Yao Xuefeng, Fang Jing, *A study of dynamic caustics around running interface crack tip*, Acta Mechanica Sinica (English Series) **15**, 182–192, 1999.

21. Shen S.-P., Nishioka T., *Theoretical development of the method of caustics for intersonically propagating interfacial crack*, Engineering Fracture Mechanics, **70**, 643–655, 2003.

22. Tomlinson R.A., Patterson E.A., *A study of residual caustics generated from fatigue cracks*, Fatigue and Fracture of Engineering Materials & Structures, **20**, 1467–1479, 1997.

23. Semenski D., *Optical method of caustics – Fulfilled experimental application to the contact problem*, Proceedings of the XVII IMEKO World Congress Metrology in the 3rd Millennium, June 22–27, 2003, Dubrovnik, Croatia, pp. 1952–1955, 2003.

24. Bakić A., Semenski D., Jecić S., *Contact caustics measurements expanded to anisotropic materials*, Archives of Civil and Mechanical Engineering, **11**, 497–505, 2011.

25. Patterson E.A., Whelan M.P., *Tracking nanoparticles in an optical microscope using caustics*, Nanotechnology, **19**, 105502 (7pp), 2008.

26. Semenski D., *Method of caustics in fracture mechanics of mechanically anisotropic materials*, Engineering Fracture Mechanics, **58**, 1–10, 1997.

27. Semenski D., Jecić S., *Experimental caustics analysis in fracture mechanics of anisotropic materials*, Experimental Mechanics, **39**, 177–183, 1999.

28. Yao Xuefeng, Zhao Hong Ping, Yeh Hsien-Yang, *Dynamic caustic analysis of propagating Mode II cracks in transversely isotropic material*, Journal of Reinforced Plastics and Composites, **24**, 657–667, 2005.

29. Kezhuang Gong, Zheng Li, *Caustics method in dynamic fracture problem of orthotropic materials*, Optics and Lasers in Engineering, **46**, 614–619, 2008.

30. Yao Xuefeng, Xu Wei, Bai Shulin, Yeh, Hsien-Yang, *Caustics analysis of the crack initiation and propagation of graded materials*, Composites Science and Technology, **68**, 953–962, 2008.

31. Gong Kez Huang, Li Zheng, Qin Wei Hong, *Influence of loading rate on dynamic fracture behavior of fiber-reinforced composites*, Acta Mechanica Solida Sinica, **21**, 457–460, 2008.

32. Gdoutos E.E., *Stress Triaxiality at Crack Tips Studied by Caustics*, Recent Advances in Mechanics, Gdoutos E.E., Kounadis A.N. [Eds.], pp. 383–396, Springer, 2011.

33. Younis N.T., *Designing an optical mechanics experiment*, World Transactions on Engineering and Technology Education, **9**, 137–144, 2011.

34. Carazo-Alvarez J., Patterson E.A., *A general method for automated analysis of caustics*, Optics and Lasers in Engineering, **32**, 95–110, 1999.

35. Theocaris P.S., Razem C., *Error analysis in evaluating SIFs by reflected caustics*, International Journal of Mechanical Sciences, **23**, 275–284, 1981.

36. Rossmanith H.P., *The influence of geometrical imperfections in the method of caustics*, Engineering Fracture Mechanics, **18**, 903–908, 1983.

37. Wallhead I.R., Gungor S., Edwards L., *Optimisation of the optical method of caustics for the determination of stress intensity factors*, Optics and Lasers in Engineering, **20**, 109–133, 1994.

38. Konsta-Gdoutos M., Gdoutos E.E., *Guidelines for applying the method of caustics in crack problems*, Experimental Techniques, **16**, 25–28, 1992.

39. Rosakis A.J., Zehnder A.T., *On the method of caustics: An exact analysis based on geometrical optics*, Journal of Elasticity, **15**, 347–367, 1985.

40. Spyropoulos C.P., *Stress intensity factor determination error by the method of caustics*, Theoretical and Applied Fracture Mechanics, **35**, 179–186, 2001.

41. Muskhelishvili N.I., *Some Basic Problems of the Mathematical Theory of Elasticity*, Groningen, Noordhoff, 1963.

42. Theocaris P.S., Pazis D.N., *Some further properties of caustics useful in mechanical applications*, Applied Optics, **20**, 4009–4018, 1981.

43. Manogg P., *Investigation of the rupture of a plexiglas plate by means of an optical method involving high-speed filming of the shadows originating around holes drilled in the plate*, International Journal of Fracture, **2**, 604–613, 1966.

44. Raptis K., Papadopoulos G.A., Costopoulos T.N., Tsolakis A.D., *Experimental study of load sharing in roller bearing contact by caustics and photoelasticity*, American J. Engineering and Applied Sciences, **4**, 294–300, 2011.

45. Yang R., Yue Z., Sun Z., Xiao T., Guo D., *Dynamic fracture behavior of rock under impact load using the caustics method*, Mining Science and Technology, **19**, 79–83, 2009.

46. Kourkoulis S.K., Markides Ch.F., Bakalis G., *Smooth elastic contact of cylinders by caustics: the contact length in the Brazilian-disc test*, Archives of Mechanics, **65**, 4, 313–338, 2013.

Received March 29, 2013; revised version July 11, 2013.